Article

Not peer-reviewed version

Rifampicin Loaded PLGA/Alginate Grafted pNVCL-Based Nanoparticles for Wound Healing

Tudor Bibire , Daniel Vasile Timofte , Radu Dănilă , Alina Diana Panainte * , Cătălina Natalia Yilmaz * , Nela Bibire , Luminita Agoroaei , Cristina Mihaela Ghiciuc

Posted Date: 19 September 2024

doi: 10.20944/preprints202409.1365.v1

Keywords: alginate; NVCL; nanoparticle; rifampicin; IC50; wound healing

Article

Rifampicin Loaded PLGA/Alginate Grafted pNVCL-Based Nanoparticles for Wound Healing

Tudor Bibire [1], Daniel Vasile Timofte [2,3], Radu Dănilă [2,3], Alina-Diana Panainte [4,*], Cătălina Natalia Yilmaz [5,*], Nela Bibire [4], Luminita Agoroaei [6] and Cristina Mihaela Ghiciuc [7,8]

[1] Doctoral School, "Grigore T. Popa" University of Medicine and Pharmacy, 16 Universitatii Street, 700116 Iasi, Romania
[2] Department of Surgery, Faculty of Medicine, "Grigore T. Popa" University of Medicine and Pharmacy, 16 Universitatii Street, 700116 Iasi, Romania
[3] "St. Spiridon County Clinical Emergency Hospital, 1 Independentei Blvd., 700111 Iasi, Romania
[4] Department of Analytical Chemistry, Faculty of Pharmacy, "Grigore T. Popa" University of Medicine and Pharmacy, 16 Universitatii Street, 700116 Iasi, Romania
[5] Biochemistry Division, Department of Chemistry, Faculty of Science, Dokuz Eylül University, Kültür Mah. Cumhuriyet Bulv. No:144 Alsancak, 35210 Izmir, Turkey
[6] Department of Toxicology, Faculty of Pharmacy, "Grigore T. Popa" University of Medicine and Pharmacy, 16 Universitații Street, 700116 Iasi, Romania
[7] Department of Pharmacology, Faculty of Medicine, Clinical Pharmacology and Algeziology, Grigore T. Popa University of Medicine and Pharmacy, 16 Universitatii Street, 700116 Iasi, Romania
[8] St. Maria Clinical Emergency Hospital for Children, 62 Vasile Lupu Street, 700309 Iasi, Roman
* Correspondence: alina.gudruman@umfiasi.ro (A.-D.P.); catalinanatalia.yilmaz@deu.edu.tr (C.N.Y.)

Abstract: The topical therapy with rifampicin (RF)-based formulations is beneficial to treat infections and to healing the wounds. Despite recent research highlighting the antibiotic's significant anti-inflammatory properties, limited topical wound healing products are currently available. Present study aimed to prove that the newly synthesized nanoparticles based on grafted alginate and poly(N-vinylcaprolactam (pNVCL) and poly-lactic-co-glycolic acid (PLGA) contributes to the healing process of a wound. The methods used were at first the synthesis of the copolymer of alginate and pNVCL via grafting from technique and radical polymerization followed by water-in-oil-in water (W/O/W) emulsification by using as oil phase PLGA dissolved in dichloromethane (DCM). The formed nanoparticles were than characterized. The loaded RF was determined to be 160 μg/mL for a 20 mg formulation and within a four-hour time frame approximately 10% of the total loaded amount was released. The inhibitory concentrations (IC50) were 192 μg/mL for the nanoparticle, 208 μg/mL for pure rifampicin, and 718 μg/mL for the rifampicin-loaded nanoparticles. Considering the double role Rifampicin was used for, the result was considered satisfactory in the way that these formulations could be used more with the wound irrigation post-surgery to avoid infections and to contribute to the healing.

Keywords: alginate; NVCL; nanoparticle; rifampicin; İC50; wound healing

1. Introduction

Wound care is becoming increasingly complex with the advent of advanced wound technology. However, the core of effective wound care can be distilled into five fundamental principles: wound assessment, wound cleansing, timely dressing changes, selection of appropriate dressings, and the use of antibiotics. Knowing the characteristics of an ideal wound dressing can help wound care specialists and clinicians in the selection of an appropriate dressing [1]. Surgical procedures are procedures that involve incisions with specialized instruments in an operating theatre, often requiring anesthesia and/or respiratory support. Surgical materials, including adhesives, sealants,

 doi:10.20944/preprints202409.1365.v

hemostatic agents, wound covers, absorptive sponges, and sutures, are expected to meet specific criteria for a good wound management. They should be non-toxic, biocompatible, and supportive of cellular proliferation for tissue regeneration, while also possessing sufficient mechanical and physical properties for durability. Most surgically sutured wounds are acute wounds that heal without complication in an expected time frame. When the incision is closed primarily, the wounds proceed through a specific cell and biochemical sequence of healing that comprises overlapping stages of hemostasis, inflammation, granulation, and epithelialization within 48 h [2].

Biopolymers, such as alginate (AgA), chitosan (Cs), collagen (Col), hyaluronic acid (HA), and silk fibroin (SF), are extensively used in wound management due to their biocompatibility, biodegradability, and similarity to macromolecules recognized by the human body. However, most of the formulations based on biopolymers still show various issues; thus, strategies to combine them with molecular biology approaches represent the future of wound healing. Naturally sourced biopolymers, which are biological macromolecules metabolized within the body, unlike synthetic polymers, do not cause chronic inflammatory or immunological reactions or toxicity due to their similarity to the extracellular matrix. A proper modification of structure or processing conditions towards functional biopolymers can alleviate some of their drawback such as poor solubility, lower producibility, poor mechanical properties, etc. but highlighting their advantages over synthetic polymers, including a well-defined and more intricate structure, biocompatibility, functionality, degradability, and renewability [3,4].

Among the biopolymers, alginic acid, a polysaccharide extracted from brown seaweeds, with distinct physical properties that make it valuable as a rheology modifier in various applications such as food products, paper consumables, printing inks, and biomaterials for medical and pharmaceutical preparations. Alginates are copolymers comprised of repeating units of guluronic acid (G) and β-D-mannuronic acid (M), linked via 1,4 glycosidic bonds. In molecular terms, they are C5 epimers of each other. The orientation of the carboxyl group (–COOH) on the C5 carbon of the six-membered saccharide ring is above the plane of the ring in the M unit and below the plane in the G unit. The polymer chain of alginate contains blocks of guluronic acid, mannuronic acid, and alternating sequences thereof. The viscosity and gel-forming capacities are key characteristics of alginate, heavily influenced by the block structure and chain length.

Alginate has been the most recognized material for cell encapsulation [5], providing immune protection and allowing good metabolic functionality in a 3D culturing environment [6–8]. Laurén et al. [9] reported that nanofibrillar cellulose may improve an alginate hydrogel's structural fidelity, preventing the collapse of printed shapes. The designed characteristics were the shear thinning ability of NFC and alginate, as they can enable the hydrogel's injectability, and thus, to prepare NFCA nanocomposites-based threads and suture coatings. Among the important strategies to improve and to design the characteristics of biopolymers is to modify them according to the desired features. More particularly, modification strategies have been employed to obtain a self-assembly behaviour up to temperature or other external stimuli such as pH, glucose level, magnetic field, etc. [10–14]. A good strategy for biopolymer modification is the grafting technique. Attaching the desired functional groups to give the desired response of the macromolecule. The resulting grafted polymer has a new set of properties that can be tailored for specific applications; more specifically, in the pharmaceutical industry, graft copolymer has shown its potential for use in drug delivery systems. The graft technique is also used to modify the surface properties of implants and medical devices, such as increasing their hydrophilicity or increasing their resistance to bacterial adhesion [15].

Among the monomers that can be used to induce thermoresponsive properties on the side chains of a biopolymer via grafting are the ones that exhibit Lower Critical Solution Temperature (LCST) close to physiological conditions such as poly(N-isopropylacrylamide and poly(N-vinylcaprolactam). Ward et al. [16] reviewed the use of polymers that present an LCST and their applications in biomedical field. They listed as the most common being poly(N-isopropyl acrylamide) (PNIPAAm) with a lower critical solution temperature, LCST of around 32°C, which is relevant for biomedical applications being close to the body temperature (37°C). The adjustment of the LCST of PNIPAAm or other monomer (e.g., poly(N,N-diethylacrylamide) (PDEAAm) - LCST over the range

 doi:10.20944/preprints202409.1365.v

of 25 to 32°C, pNVCL with LCST between 25 and 35°C, poly [2-(dimethylamino)ethyl methacrylate] (PDMAEMA) with an LCST of around 50°C, poly(ethylene glycol) (PEG), whose LCST is around 85°C) can be achieved by copolymerizing with hydrophilic or hydrophobic monomers rendering the overall hydrophilicity of the polymer higher or lower respectively.

Poly(N-vinylcaprolactam) (pNVCL) is a water-soluble, non-toxic, thermosensitive, and biocompatible polymer categorized under N-vinylamide polymers. In comparison, although poly(N-isopropylacrylamide) (PNIPAAm) is extensively studied as a thermosensitive polymer, PNVCL exhibits even higher biocompatibility due to the direct linkage of the amide group to the hydrophobic backbone chain (C–C). Consequently, the hydrolysis of the amide group in PNVCL does not yield small amide compounds, which are undesirable for biomedical applications and limit the biocompatibility of PNIPAAm [17]. The combination with biocompatible monomers such as N-vinylcaprolactam with alginate can lead to functional biocompatible materials which impart both the characteristics of alginate and NVCL.

Present study deals with the exploration of the potential of the copolymers of alginate with N-vinylcaprolactam synthesized via graft copolymerization and formulated as nanoparticles by coating with poly (D, L-lactide-co-glycolide (PLGA) shell. The characteristics of the AgA-pNVCL matrix will be explored as sealant materials for surgical sutures. The motivation for formulating the copolymer with a shell of PLGA is to achieve a smaller burst release and prolonged cumulative release. PLGA offers the advantage of controlling the release of the incorporated drug along with achieving a very small particle size being in the same time a biocompatible material [18].

2. Materials and Methods

2.1. Chemicals

Alginic acid sodium salt powder (AgA, Sigma Aldrich, Saint Louis, USA) was utilized, along with N-vinylcaprolactam (NVCL), as monomer, achieved from Sigma Aldrich. The initiator system comprised ammonium persulphate (APS, Sigma Aldrich) and 50% hydrogen peroxide solution. The reaction was carried out in ultra-pure distilled water as the solvent. To create the nanoparticle suspension, a 0.5 wt.% acetic acid glacial solution was employed. Purification of the copolymer was achieved using a dialysis bag with a cut-off of 3.5 kDa. Rifampicin (RIF), 99% purity, with a molecular weight (Mw) of 822.95 g/mol sourced from S.C. Antibiotice S.A., Iasi, Romania. Poly(D,L-lactide-co-glycolide) 50:50 (PLGA), Sigma Aldrich product was used to form the nano/microparticles. All other chemicals and reagents used in this study met analytical grade standards or exceeded them and were procured commercially.

2.2. Preparation of Grafted Biopolymer

The grafted biopolymer i.e., alginate grafted N-vinylcaprolactam (NVCL) was synthesized by using initiator system comprised ammonium persulphate (APS, Sigma Aldrich, Saint Louis, USA) and 50% hydrogen peroxide solution under nitrogen flow within a ratio of 0.1% against the monomer (NVCL).

2.3. Preparation of PLGA Coated Alginate Grafted from NVCL

The prepared biopolymeric matrix was used further to synthesize nano/microparticles without and containing Rifampicin, the selected drug model for post-surgery wound healing.

An amount of prepared biopolymer was dissolved in water within a concentration of 0.1 wt.% and then Rifampicin was added to the polymeric solution to ensure a good blending and formation of electrostatic bonds with the hydrophilic groups of the biopolymer. The theoretical amount used for the Rifampicin loading within the matrix was 0.5 wt.% against the polymer amount. The mixture was stirred for couple of hours then lyophilized.

The biopolymeric matrix without Rifampicin was dissolved in twice distilled water within a concentration of 0.1 wt.%. The oil phase solution was prepared by dissolving 0.1 g PLGA (50/50) in dichloromethane (DCM) and Span 80 was added to ensure a good stability of the emulsion. The oil

 doi:10.20944/preprints202409.1365.v

phase was probe sonicated for 10 minutes then the water phase was added dropwise under strong stirring under vortex to prepare water-in oil emulsion. The first emulsion was again probe sonicated and then added dropwise in the second water phase consisting of 5 wt.% polyvinyl alcohol low molecular weight, Tween 80 and salt to give the final water-in-oil-in water (W/O/W) dispersion. The solvent was evaporated at room temperature, and the system was kept under stirring overnight. The final dispersion was then centrifugated at 15000 rpm under a temperature of 5°C to collect the nano/microparticles of **poly(**N-vinylcaprolactam) grafted alginate (AgA-g-pNVCL) coated with PLGA.

The formation of particles containing Rifampicin was performed similarly except the fact that in the water was dissolved the matrix loaded with Rifampicin. The drug content was determined using high-performance liquid chromatography (HPLC) and it was reported in our previous work [4] as being 160 μg/mL in 20 mg formulated sample.

2.4. Fourier Transform Infrared Spectroscopy (FTIR) Analysis

The structure was confirmed by FT-IR spectra of the copolymer films which were recorded with a Perkin-Elmer Spectrum-100 ATR-FTIR instrument (Shelton, USA) by scanning in the range of 600-4000 cm^{-1}.

2.5. Particle Size Analysis

The average particle size and particle size distribution of the final nanoparticles loaded with rifampicin was measured by NanoZS model (Malvern Instruments, Grovewood, UK) zetasizer instrument. The sample was prepared by diluting the solution of the dissolved samples 5000 times with distilled water.

2.6. Differential Scanning Calorimetry (DSC)

The observed phase changes such glass transition temperatures DSC analysis were performed on dried substances (approximatively 5 mg) using a Perkin Elmer Diamond DSC instrument (Grovewood Rd, United Kingdom) at a heating rate of 10°C/min under N2 atmosphere from 20 to 250°C.

2.7. Scanning Electron Microscopy (SEM)

The scanning electron microscopic (SEM) images of the cross-section of the lyophilized formulations were captured using a Carl Zeiss 300 Sigma VP model equipped with Gemini Optical Technology (Los Angeles, USA). Magnification is given in the figures.

2.8. In Vitro Release Study of Formulations

The dialysis bag diffusion technique was used to study the in vitro drug release of RF from lyophilized nanoparticles. Samples in dried state were weighed, placed in the dialysis bag (cellulose membrane, molecular weight of 12,000–14,000 Da), hermetically sealed and immersed in 100 mL of Phosphate Buffer (pH = 7.4). The entire system was kept at 37 ± 0.5°C with continuous magnetic stirring at 300 rpm. Samples were withdrawn from the receptor compartment at predetermined time intervals and the entire receptor phase was replaced with fresh medium at 37 ± 0.5°C to obtain sink conditions. The amount of drug that was released was then determined by the described HPLC method. The experiments were carried out in triplicate.

The evaluation of drug release kinetics, Korsmeyer–Peppas semi-empirical Equation (1) was applied for the initial release stages (~60% fractional release) [19,20]:

$$\frac{M_t}{M_\infty} = k_r \cdot t^{n_r} \quad (1)$$

where $\frac{M_t}{M_\infty}$ is the fractional drug released, M_t and M_∞ are the cumulative drug released amounts at time t and at equilibrium, respectively (or experimental maximum released amount taken at the

 doi:10.20944/preprints202409.1365.v

plateau of the release curves), k_r is rate constant dependent on the characteristics of the drug loaded system and n_r is the diffusional exponent which defines the type of the release mechanism. A value of n_r~0.5 is characteristic of the Fickian diffusion mechanism of the drug from the biopolymeric matrix; the values in interval $0.5 < n_r < 1$ are specific to an anomalous or non-Fickian behaviour. A case II of transport mechanism occurs when $n_r = 1$, which means zero-order kinetics, while a special case II of transport mechanism is indicated by values $n_r > 1$ [19,20].

2.9. Cytotoxicity Studies

For the determination of the cytotoxicity and IC50 values of pure active substances and formulations, MTT assay was performed. The purpose of the tests was to evaluate the cytotoxic effect of different concentrations of active substances and formulations on 3T3-L1 cell lines; 3T3-L1 cells are derived from 3T3 cells and have a fibroblast-like morphology, but, under appropriate conditions, they differentiate into an adipocyte-like phenotype. The following solutions were prepared and used during the experiments:

Complete Medium (DMEM: F12 + 10%FBS +1%Pen-Strep): to prepare 50 mL of complete medium, the medium 45 mL of DMEM: F12 (obtained from Gibco Cat No: 11320033), 5 mL of fetal bovine serum (FBS) (obtained from Gibco Cat No: 10500064) and 500 µL of Pen-Strep (obtained from Gibco Cat No: 15070063) was to a 50 mL sterile falcon in a biolaminar safety cabinet. In the experiments, the need was prepared quite freshly.

171 µM Triton-X solution (Positive Control): 235 µL of 4263 mM stock Triton-X (obtained from Sigma-Aldrich Cat No: X100-100ML) solution was added onto 765 µL medium. The concentration of the solution thus obtained is 1000 mM. Then, 1 µL of the 1000 mM intermediate stock was taken and added to 999 µL medium and a second 1000 µM intermediate stock was obtained. Finally, 171 µL of 1000 µM intermediate stock was taken and added to 829 µL medium, and 171 µM Triton-X solution was obtained. Finally, it was sterilized by filtration through a 0.22 µm membrane filter.

Sterile PBS: two of the PBS tablets (from Thermo Scientific Cat No: P4417-100TAB) were dissolved in 400 mL water and then sterilized in an autoclave device.

70% EtOH: it was prepared with the action of 96% EtOH to be used in routine cleaning processes. For this, it was prepared by mixing 365 mL of 96% EtOH with 135 mL of distilled water for 500 mL of solution.

Rifampicin Solutions: 16 mg of rifampicin was weighed and dissolved in 100 µL of DMSO, and the concentration of the resulting solution was found to be 160,000 µg/mL. By taking 5 µL of this solution and adding it to 995 µL medium, a solution with a concentration of 800 µg/mL (DMSO 0.5%) was obtained, and solutions with concentrations of 400, 200, 100, 50, 25 and 12.5 µg/mL were obtained with 2-fold serial dilutions.

Nanoparticles Solution: 20 mg of nanoparticles were weighed and dissolved in 100 µL of DMSO. The concentration of the obtained solution was obtained as 200,000 µg/mL. 5 µL of this solution was added to 995 µL of medium and the concentration of the resulting solution was found to be 1000 µg/mL (0.5% DMSO). Based on this solution, solutions with concentrations of 500, 250, 125, 62.5 and 31.25 µg/mL were obtained with 2-fold serial dilutions.

Rifampicin Loaded Nanoparticles Solution: 20 mg rifampicin loaded nanoparticle was weighed and dissolved in 100 µL of DMSO. The concentration of the obtained solution was obtained as 200,000 µg/mL. 5 µL of this solution was added to 995 µL of medium and the concentration of the resulting solution was found to be 1000 µg/mL (0.5% DMSO). Based on this solution, solutions with concentrations of 500, 250, 125, 62.5 and 31.25 µg/mL were obtained with 2-fold serial dilutions.

2.10. Scratch Assay

The scratch assay was performed according to the procedure applied by Orsu et al. [21]. The method was based on the observation that, upon creation of a new artificial gap, so-called scratch, on a confluent cell monolayer, the cells on the edge of the scratch will move toward the opening to close the scratch until new cell-cell contacts are established again [22]. As mentioned, for the MTT cell viability assay, 3T3-L1 fibroblast cells were used for the scratch assay as well. In the experiment, the

 doi:10.20944/preprints202409.1365.v

cells were plated either in 10% FBS containing cell culture medium or 1% FBS containing cell culture medium. First, we compared the relevancy/appropriateness of these two different FBS concentrations. Second, the same test subjects in the former assay, rifampicin, nanoparticles, rifampicin-loaded nanoparticles, were separately tested in scratch assay in the presence of medium control whether they alter the scratch closure rate compared to the control and to each other. This has been done by capturing the image of the scratch in the beginning (0th hr.), and in the following 12th, 24th, and 30th h time points. Microscopic scratch images were used to calculate the closure of the gaps in time by using the Image J software. The potential statistical significances between the percentages of different test subjects at the same time-points, and between the percentages of the same test subject at the different time-points were tested by two-way, and one-way ANOVA, respectively. The final statistical significance between the two test subjects in terms of wound-healing efficiency was tested again by one-way ANOVA. In this evaluation, Tukey's multiple comparisons test was used to determine which groups are significantly different to each other.

3. Results and Discussions

3.1. Matrix Characterization

3.1.1. FTIR Spectroscopy

Spectroscopy tests were performed to detect either the appearance of new chemical bonds or the modification of existing ones, which can be attributed to possible interactions between grafted alginate (AgA-g-pNVCL) and polylactide-glycolide (PLGA) to form NPs by compared with their pure constituents (AgA; PLGA and AgA-g-pNVCL). The obtained spectra were represented in Figure 1.

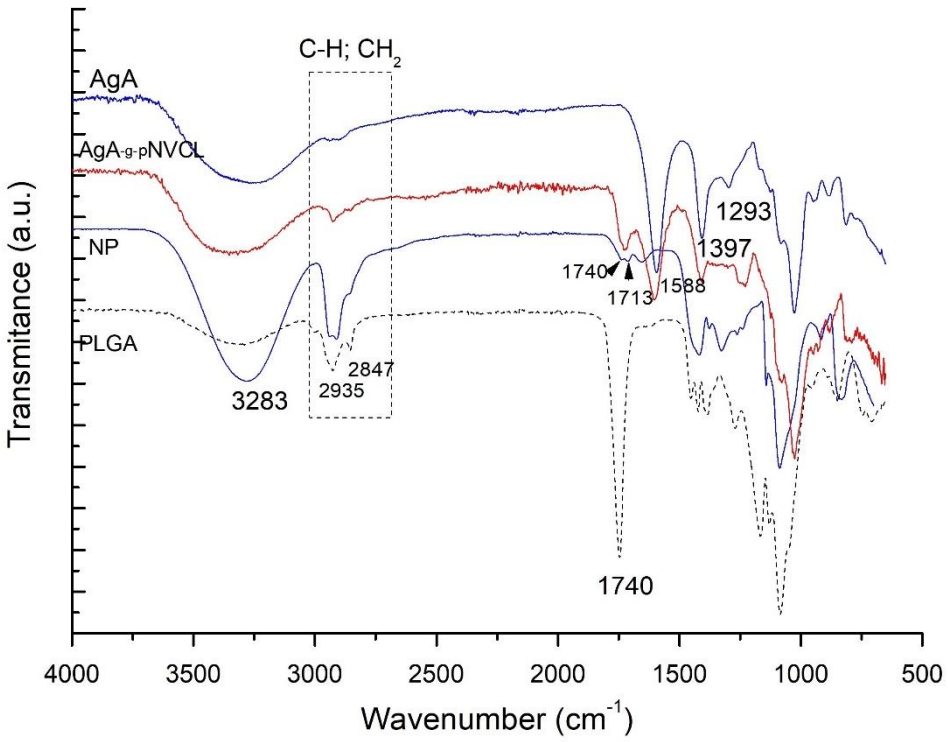

Figure 1. FTIR spectra of the prepared NPs and their components.

The purpose of the spectra analysis was to confirm the structural identity of the grafted copolymer and the nanoparticle formation of PLGA/AgA-g-pNVC. The grafted copolymer's structural identity has been reported in detail in our publication [4]. By combining the grafted copolymer of alginate with PLGA as coating shell, it was expected that the spectra of the final nanoparticle to consist of both, the specific vibration bands from the alginate-based copolymer and PLGA. The formation of new vibration bands and/or shifts to lower or higher peaks within the

 doi:10.20944/preprints202409.1365.v

spectrum range are expected to occur. The spectra of PLGA contained a strong peak at 1094 cm^{-1} specific for C–O–C stretching, as well as a peak at 1740 cm^{-1} for C=O stretching. By analysing the spectrum of the NP, the specific peak of C-O-C from PLGA was found at 1086 cm^{-1} even though alginate-based matrix also contains peak at 1020 cm^{-1} thanks to the presence of -C-O- of the glucoside moieties indicating the presence of PLGA moieties. The peaks of CH, CH_2 stretching vibrations from 2900-2800 cm^{-1} were observed to be more intense sign that the conjugate between PLGA and alginate matrix was formed. Moreover, the peak at 3282 cm^{-1} of OH groups is increased as intensity and is wider, indicating the formation of the conjugate and the interactions between the two polymers via H-bonding.

3.1.2. Particle Size Analysis

The particle size of the formed nanoparticles was measured (Figure 2) and from the size distribution and intensity it was determined that the formed particles have nanosize dimensions up to particle type. It was found that the unloaded particles had a narrow distribution with an average of 103 nm size while the ones loaded with Rifampicin (RF) showed a wider distribution but a unimodal peak with an average size distribution of 201 nm; this outcome confirmed the loading within the polymeric matrix.

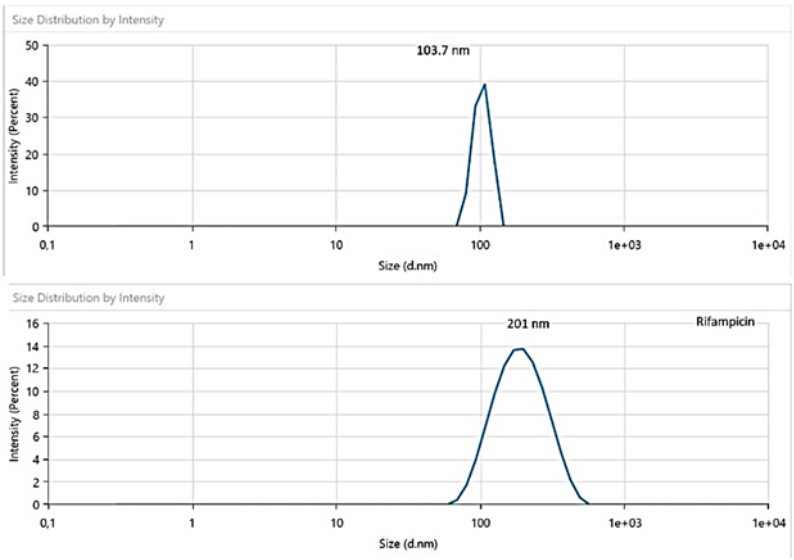

Figure 2. Particle size distribution for the nanoparticles without Rifampicin (the upper graph) and loaded with Rifampicin (downward).

3.1.3. DSC Analysis

Thermal properties of the polymeric nanoparticles with and without RF were tested to check the presence of the drug within the matrix and to determine the thermal stability and homogeneity of the prepared formulations. Figure 3 presents the DSC thermograms of pure RF, polymeric nanoparticles with and without RF.

 doi:10.20944/preprints202409.1365.v

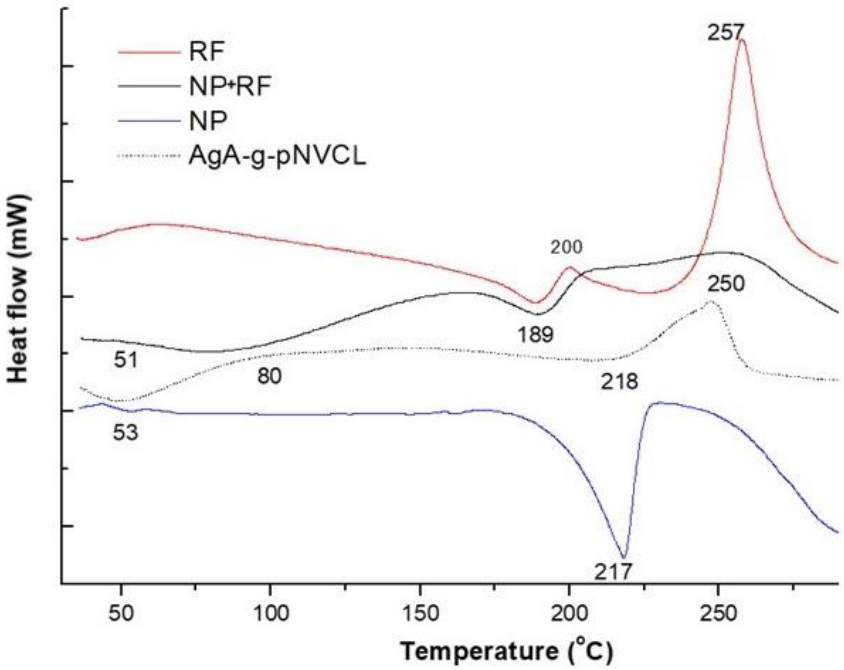

Figure 3. DSC thermograms of polymeric nanoparticles with and without RF.

As represented within Figure 3, pure rifampicin (RF) showed a melting peak at 189^{0}C being in line with the data reported in literature [23]. As the used Rf was a commercial sourced one, the DSC thermogram of RF, form II, showed an exo-endothermic process at 189°C-200°C, leading to a product that decomposes at 257°C. The presence of the same peaks was determined also in the thermogram of the polymeric matrix loaded with RF (NP+RF), being identified endo-thermic peaks around 189°C and 250°C. Liu et al. [24] also found out that RF had an exothermic crystallization peak at 213°C and a degradation peak at 249°C. The peak from 250°C almost disspeared and overlapped with the degradation peak of the polymeric matrix, indicating the fact that Rf was encapsulated. When analysing the thermogram of nanoparticles of AgA-g-pNVCL coated with PLGA (i.e., NPs) there were observed small peaks at 50°C being assigned to the glass transition of PLGA and an endothermic peak around 217°C being explained by the beginning of polymer degradation. Comparable results were found by Rao et al. [25]. They found for sodium alginate a broad endothermic peak around 100°C and a sharp exothermic peak at 250°C, the latter one being connected with its thermal decomposition. The copolymer AgA-g-pNVCL showed three thermal events at 80°C, at 218°C and 250°C. It seems that PLGA coating induced a less thermal stability of the molecule as the peak from 217°C indicates the beginning of the nanoparticles' degradation especially the PLGA attached moieties. A further degradation envised the macromolecular chains of AgA-g-PNVCL. The outcome from DSC analysis not only proved the complexity of the polymeric matrix but also confirmed the presence of RF inside and its thermal characteristics.

3.1.4. SEM Observations

SEM was used to study the surface morphology of the polymeric nanoparticles with and without RF together with the pure constituents (lyophilized hydrogel of AgA-g-pNVCL and RF). The SEM images showed that RF particles were smooth and rod-like (Figure 4d,e) whereas polymeric nanoparticles had spherical shapes and irregular due to breakage after the lyophilization process (Figure 4b,c,f).

 doi:10.20944/preprints202409.1365.v

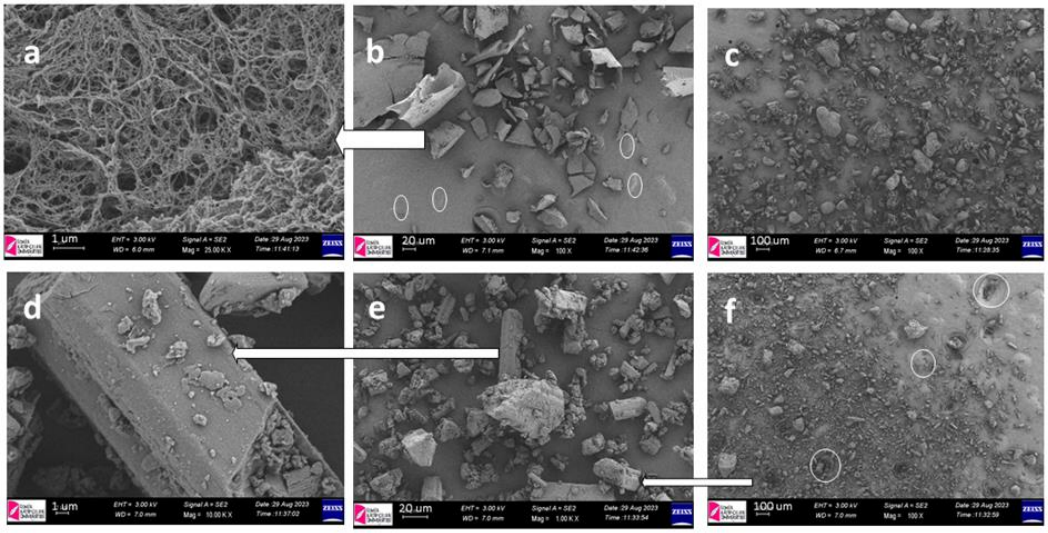

Figure 4. SEM observations for the polymeric/nanopolymeric matrix and pure RF: (a) liophylized hydrogel of AgA-g-pNVCL; (b) and (c) lyophilized nanoparticles of AgA-g-pNVCL coated with PLGA without RF at different magnifications; (d) image of RF; (e) and (f) lyophilized nanoparticles of AgA-g-pNVCL coated with PLGA with RF at different magnifications.

Even though the particles were collapsed due to the lyophilization, there can be distinguished the spherical shape and in some market places voids with rod-like shapes inside indicating the success of the encapsulation. The results from SEM were in line with DSC results confirming the expected outcome. Similar outcomes were obtained also by Snejdrova et al. [26] or by Rai et al. [27].

3.2. In Vitro Release Profile

Prior to evaluate the in vitro release behavior of rifampicin, the amount of drug trapped within the polymeric chains was determined by HPLC assay, and it was found out that 20 mg polymeric micro/nanoparticles consisted of 160 µg/mL of rifampicin as it was reported within the previous study [4]. This outcome was useful for further studies such as cytotoxicity assessment, in vitro release and wound closure capacities. Figure 5 described the in vitro release profile of Rifampicin within 7 hours from the beginning of the experiment.

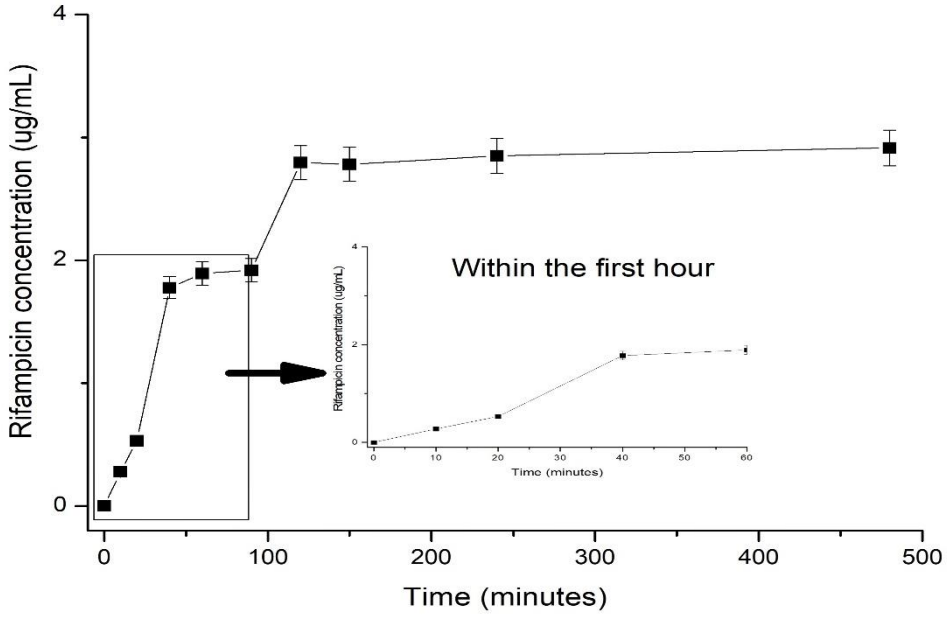

Figure 5. In vitro release profile of Rifampicin from the polymeric micro/nanoparticles of AgA-g-pNVCL/PLGA.

 doi:10.20944/preprints202409.1365.v

As shown in Figure 5, in the first 60 minutes from the administration of the formulation an amount of about 1% of the total loaded Rifampicin. As observed from the in vitro release profile, over the time interval release, the release capacity was studied, low amount of Rifampicin was determined by HPLC method. More specifically within the first hour from the administration approximatively 1% was released, following-up after another interval of 2 hours another 1% being further determined. The outcome regarding the low release of RF from various matrices was previously reported. Bibire et al. [4] found out an amount of released RF within 4 hours of 5.98 ppm while Parmar et al. [28] reported a delivered amount of RF of 10% within 10 hours in the case of encapsulated RF within liquid-crystalline folate nanoparticles. Interestingly, they reported a self-assembly behaviour to control the loading capacity of rifampicin and additionally its delivery's profile. They found out that by decreasing the particle size of the particles encapsulating Rifampicin, the loaded amount is lower. However, the low amount of Rifampicin detected within the matrix did not show significant differences as concerning its cytotoxicity activity or release profile. An additional factor reported and, which seemed to influence the release behavior is that Rifampicin when encapsulated within nanoparticles is binding via its functional groups creating internal crosslinks which may slow down the release. Within the present study Rifampicin was encapsulated within the matrix of grafted alginate with poly(N-vinylcaprolatam) and protected by a shell of PLGA. The size of formed particles was determined as being around 100 without RF and 200 nm when RF was loaded, as presented within Figure 2. The explanation on the low efficacy regarding the loading amount but also the capacity of the nanoparticle to release the trapped RF was found to be on the base of created crosslinks between RF and polymeric matrix. Another reason is also the drug's low solubility. Henwood et al. [29] reported the low solubility of Rifampicin in water and buffer system up to the content of the amorphous moiety from the raw drug and a careful selection of the drug as raw material is needed. The Rifampicin used within the study was provided from a local medicine company and according to the DSC analysis (thermogram from Figure 3) a form II of Rifampicin was determined so the polymorphism could influence the solubility in aqueous phases [30].

The drug release mechanism was assessed by the theoretical kinetic evaluation by applying the semi-empiric equation (1) of Peppas et al. [19] of the release profile within the first hour, which showed an anormal non-Fickian mechanism (case II), a matrix dependent mechanism considering the values of the release rate of 0.958 min^{-1} (R^2 = 0.9911) and n value of 0.7502, indicating that the release mechanism was case II which involves swelling and erosion of the matrix structure. Similar results for in vitro delivery of Rifampicin were found by Hiremath et al. [31].

3.3. Cytotoxicity Studies

Cytotoxicity is a crucial factor in wound dressing fabrication. More importantly, it can support skin tissue restoration. The first step of the assessment of the cytotoxicity of Rifampicin was to calculate the IC50 values. The cytotoxicity data about rifampicin was limited. In a study by Saravanan et al., the IC50 value of rifampicin was found to be 87 μg/mL. For the assessment, human monocyte cells (THP-1) were used, the cells were incubated with rifampicin for 72 hours, and then measured the cytotoxicity with Alamar blue [32]. Within the present study, the IC50 value for rifampicin was found to be 208.8 μg/mL for 3T3-L1 cell line. Cells were incubated with rifampicin for 24 hours and cytotoxicity was measured by MTT assay. The differences between the two tests, were primarily, the cell type and then also incubation time, obviously resulted in different IC50 values. As the proposed formulations are intended to be used within the external use on wounds, so the most relevant cell type to be tested was decided to be 3T3-L1. Figure 6 described the cytotoxicity results and the IC50 values calculated for all studied samples.

 doi:10.20944/preprints202409.1365.v

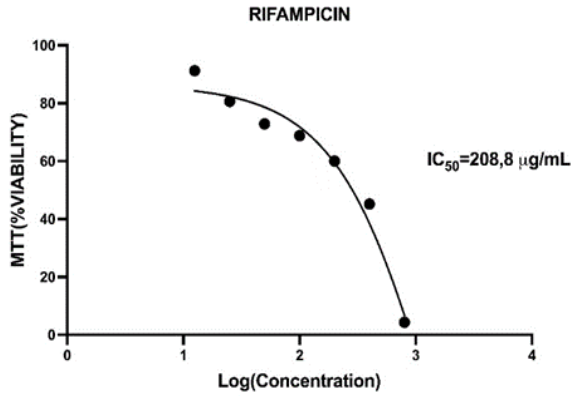

(a)

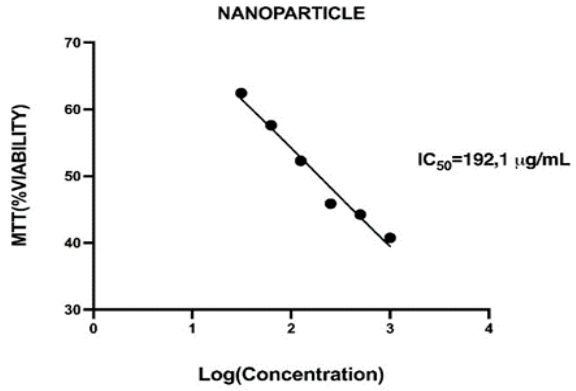

(b)

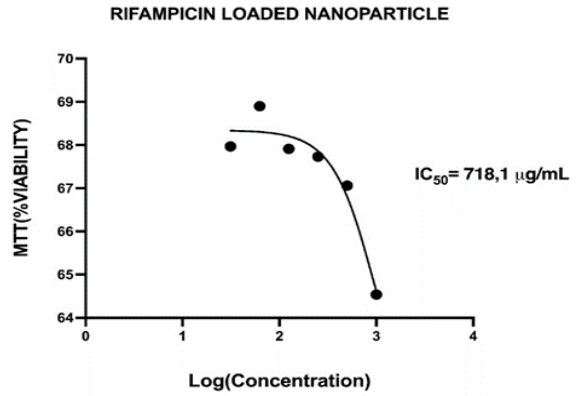

(c)

Figure 6. Cell viability test's results for the studied samples: (a) pure Rifampicin; (b) synthesized nanoparticles (AgA-g-PNVCL/PLGA); (c) Rifampicin loaded nanoparticles. *Within the caption, the IC50 values were determined by applying the sigmoidal mathematical model of the program GRAPHPAD.

IC (inhibitory concentration) curves are dose-response curves used to determine the specific drug concentration required to reduce the viable cell population by a certain percentage compared to cells grown without drug exposure. The IC50, or inhibitory concentration at 50%, represents the concentration of a compound needed to inhibit a biological process by half. IC50 values are crucial in cytotoxicity assessments as they indicate the amount of a drug required to achieve this inhibition. The IC curves demonstrate changes in the population due to increased cell death or decreased cell proliferation [33]. Determining the IC50 value has significant implications beyond merely inhibiting

 doi:10.20944/preprints202409.1365.v

cell growth or increasing cell death. In cancer treatment, using certain drugs at the IC50 concentration can reduce tumor growth by half. If the IC50 is identified at a lower concentration, it indicates that the drug will be effective at lower doses, thereby reducing systemic toxicity in patients. Utilizing the IC50 concentration can effectively kill cancer cells and halt their growth while minimizing the toxic effects on healthy cells in the body. The values found for the prepared formulations were 192 µg/mL for the nanoparticle, 208 µg/mL for pure Rifampicin and the nanoparticle loaded with Rifampicin had a IC50 value of 718 µg/mL. As observed the IC50 value of the conjugate (i.e., nanoparticle of AgA-g-pNVCL/PLGA loaded with RIF) had a higher value than its constituents itself. Within the literature this phenomenon was defined as "mixture effect" [34]. From toxicological point of view, the study of the combined effects of substances is crucial because organisms are often exposed to complex mixtures of chemicals rather than single substances. When the combined effect of chemicals is greater than the sum of their individual effects, a synergetic effect of the mixture is reported. It seems that it is also the case of the present formulation, the loaded nanoparticle with Rifampicin presented a value of IC50 three times higher than its constituents. The reason behind this phenomenon needs to be investigated in further investigations up to the concentration dose and time of exposure.

3.4. Cell Scratch Assay (Wound Healing)

A cell scratch assay was used to assess the wound-healing potential of the nanoparticles-based formulations. Lower concentrations than the MTT assay were tested to avoid cytotoxic effects. During a period of 30 h, wound closure was monitored at 0-, 12-, 24- and 30-h intervals. A relative wound area (%) was determined. Figure 7 describes the development of the scratches in the presence of tested materials.

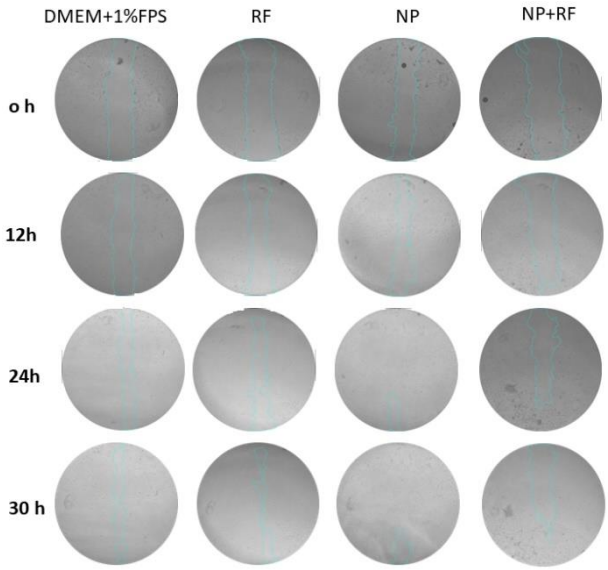

Figure 7. The microscopical observations of the closures over a period up to 30 hours.

As shown within Figure 7, the microscope images were taken at 0, 12, 24, 30 hours and % wound area was determined by using Image J software, a Java-based image processing program developed at the National Institutes of Health and the Laboratory for Optical and Computational Instrumentation. The percentage of wound area data were normalized by proportioning according to hour 0. The statistical significance of the difference between different groups at the same hours of the data showing % wound area against time was shown by two-way ANOVA test and the statistical significance of the difference between different hours of the same groups was shown by one-way ANOVA test. ANOVA test was used to investigate whether the difference between the groups in % wound healing calculated according to the formula specified in the procedure was statistically

 doi:10.20944/preprints202409.1365.v

significant. Tukey's multiple comparisons test was used to determine between which groups there was a significant difference. Figure 8 described the closure activity in time and the wound area was determined after each time interval. As observed, the activity of Rifampicin loaded within the nanoparticles was more obvious after 24 hours from the application of the nanoparticle's solution containing RF.

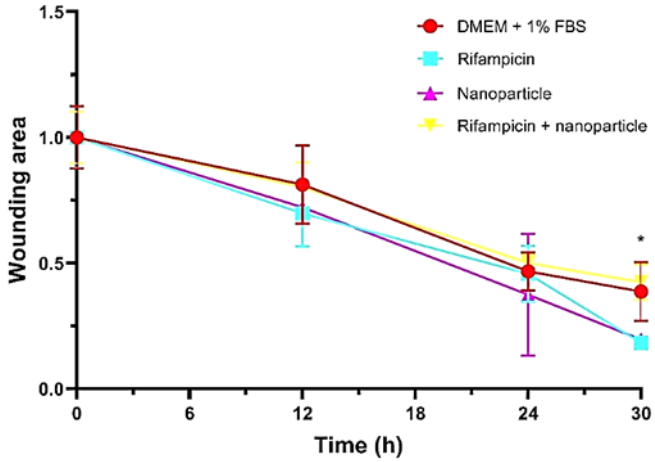

Figure 8. Wound areas of 3T3-L1 cells incubated with control (DMEM + 1%FBS), Rifampicin, nanoparticles, rifampicin + nanoparticles until 30th hour. P<0.05* indicates statistically significant difference between rifampicin and rifampicin + nanoparticles groups at 30th hour.

When the closure activity is to be compared between the tested samples (Figure 9) it can be interestingly remarked the activities of the distinct solutions of nanoparticles and Rifampicin being much higher than the complex formulation of Rf loaded inside the nanoparticles.

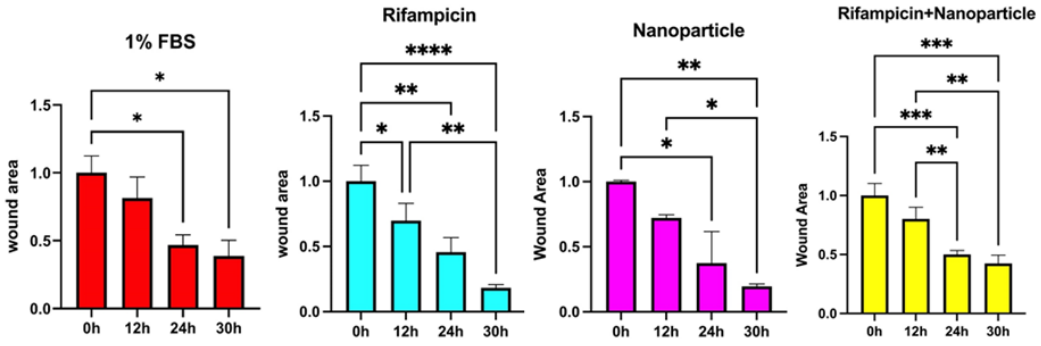

Figure 9. Wound areas of 3T3-L1 cells incubated with control (DMEM + 1%FBS), rifampicin, nanoparticles, rifampicin + nanoparticles until 30th hour. A: control, B: rifampicin, C: nanoparticles, D: rifampicin + nanoparticles groups. P<0.05*, P<0.01**, P<0.001***.

A total closure effect of 60% was determined in the case of the RF loaded nanoparticles while separate solutions of Rifampicin and nanoparticles showed around 80% (Figure 10).

 doi:10.20944/preprints202409.1365.v

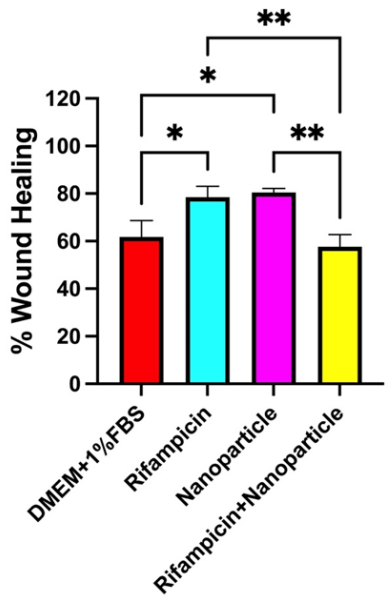

Figure 10. Wound healing as percent of 3T3-L1 cells incubated with control (DMEM + 1%FBS), Rifampicin, nanoparticles, rifampicin + nanoparticles for 30 hours. P<0.05*, P<0.01**, P<0.001*** indicated statistically significant difference between groups.

Previously reported results [35] demonstrated the capacity to proliferate the cells when hydrogels composed of the similar polymeric carrier loaded with Rifampicin. The performed scratch assay was done to test the migration and proliferation of Normal Human Dermal Fibroblasts (NHDF) within a time period of maximum 72 hours. The RF-loaded hydrogels demonstrated a synergetic effect between polymeric matrix and drug, the wound closure activity being more evident after 24 hours from exposure. However, many studies found out a poor closure activity of Rifampicin based polymeric systems, most of the studies associating the activity of Rifampicin with an antibacterial one [36] in topical treatment of surgical wounds and rifampicin-based systems may be recommended in wound site irrigation [37]. As reported, wound irrigation supposes the usage of the material as a cleaning solution to sanitize the injury/postsurgical wound and to remove the elements that affect the healing process. When done correctly, it helps to remove any extra cellular debris, surface bacteria, wound exudate, dressing residue, and residual topical agents [38].

4. Conclusions

Considering the motivation of the study of not finding enough formulations to be used as sealant materials in post-surgical wounds, a formulation based on nanoparticles formed from grafted alginate with poly(N-vinylcaprolactam) and coated with PLGA and loaded with Rifampicin (RF) was reported. Rifampicin (RF) is an antimicrobial drug which manage the and treat diverse mycobacterial infections and gram-positive bacterial infections present at wounds after surgeries. However, the topical therapy with rifampicin-based formulations seemed to be efficient not only to treat infections but also to contribute to the healing process. The newly synthesized nanoparticles based on grafted alginate and poly(N-vinylcaprolactam) and PLGA (AgA-g-PNVCL/PLGA) contribute to the healing process of a wound. The methods used were at first the synthesis of the copolymer of alginate and pNVCL via grafting from technique and radical polymerization followed by W/O/W emulsification by using as oil phase PLGA dissolved in dichloromethane (DCM). The formed nanoparticles were characterized by means of particle size showing a size of 200 nm for the particles loaded with RF, FT-IR spectroscopy proved the chemical identity of the copolymer and the conjugate. The presence of bands of each pure substance within the new product together with broadening of OH and COOH showing interactions led to the substance identification. Morphological observation performed by SEM revealed the presence of the RF particles within the polymeric network; the thermal characteristics determined by DSC indicated the presence of a form II RF which is less susceptible to

 doi:10.20944/preprints202409.1365.v

dissolution, explain its low drug loading and in vitro release profile. It seemed that due to low solubility of the drug together with susceptibility to be strongly attached to the polymeric matrix via H bonds, a low released amount of RF was determined approximatively 10% within 4 hours from the administration. However, the analysis of the kinetics of the release profile, the delivery process was based more on a non-Fickian mechanism up to the erosion of the polymeric matrix. The cytotoxicity by MMT assay of the tested formulations (pure RF, unloaded nanoparticles and RF loaded nanoparticles) revealed the non-toxic character of the formulations, and the inhibitory concentrations (IC50) were determined of 192 μg/mL for the nanoparticles, 208 μg/mL for pure Rifampicin and 718 μg/mL for the nanoparticles loaded with Rifampicin. Wound closure capacity was assessed via in vitro scratch assay and it was found out a total of 60% closure for the prepared RF loaded nanoparticles. Considering the double role Rifampicin was used for, the result was considered satisfactory in the way that these formulations could be used more with the wound irrigation post-surgery to avoid infections and to contribute to the healing.

The main limitation of the study consisted of not having enough case studies regarding the usage of Rifampicin entrapped within polymeric nanoparticles to compare the results and to make a fair opinion. However, the obtained in vitro results for the delivery capacity and the wound healing ability are to be studied further in vivo environment.

Author Contributions: Conceptualization, T.B., C.M.G., C.N.Y., D.V.T. and R.D.; validation, N.B. and L.A.; investigation, T.B., C.N.Y. and A.D.P.; resources, T.B. and N.B.; writing—original draft preparation, T.B. and C.N.Y.; writing—review and editing, D.V.T., A.D.P. and C.N.Y. All authors have read and agreed to the published version of the manuscript.

Funding: This research received no external funding.

Data Availability Statement: The data presented in this study are available on request from the corresponding authors.

Acknowledgments: The authors acknowledge the company S.C. Antibiotice S.A. Iasi, Romania for supplying the substance Rifampicin. T.B. acknowledges the "Grigore T. Popa" University of Medicine and Pharmacy, Iasi, Romania and the Doctoral School for partial supply of chemicals and materials and for support in performing some analyses of the study.

Conflicts of Interest: The authors declare no conflicts of interest.

References

1. Akagi, I.; Furukawa, K.; Miyashita, M.; Kiyama, T.; Matsuda, A.; Nomura, T.; Makino, H.; Hagiwara, N.; Takahashi, K.; Uchida, E. Surgical wound management made easier and more cost-effective. *Oncol. Lett.* **2012**, *4* (1), 97-100.
2. Mangram, A.J.; Horan, T.C.; Pearson, ML, Silver, L.C.; Jarvis, W.R. Guideline for prevention of surgical site infection, 1999. Centers for Disease Control and Prevention (CDC) Hospital Infection Control Practices Advisory Committee. *Am. J. Infect. Control*. **1999**, *27*, 97-132. Quiz 133-134; Discussion 96.
3. Bibire, T.; Yilmaz, O.; Ghiciuc, C.M.; Bibire, N.; Dănilă, R. Biopolymers for Surgical Applications. *Coatings* **2022**, 12, 211.
4. Bibire, T.; Ghiciuc, C.M.; Yilmaz C.N.; Ursu, R.G.; Dănilă R. The Development of Alginate Based Matrices Loaded with Rifampicin for Wound Healing. *Med. Surg. J.* **2024,** *128* (1), 167-176.
5. Hunt, N.C.; Grover, L.M. Cell encapsulation using biopolymer gels for regenerative medicine. *Biotechnol Lett* **2010**, 32, 733–42.
6. Lim, F.; Sun, A.M. Microencapsulated islets as bioartificial endocrine pancreas. *Sci.* **1980,** *21*, 210(4472): 908-910.
7. Khattak, S.; Chin, K.S.; Bhatia, S.R.; Roberts, S.C. Enhancing oxygen tension and cellular functionin alginate cell encapsulation devices through the use of perfluorocarbons. *Biotechnol. Bioeng.* **2007**, *96*, 156-66.
8. Tan, W.H.; Takeuchi, S. Monodisperse alginate hydrogel microbeads for cell encapsulation. *Adv. Mater* **2007**, *19*, 2696–701.
9. Laurén, P.; Somersalo, P.; Pitkänen, I.; Lou, Y.R.; Urtti, A.; Partanen, J.; Seppälä, J.; Madetoja, M.; Laaksonen, T.; Mäkitie, A.; Yliperttula, M. Nanofibrillar cellulose-alginate hydrogel coated surgical sutures as cell-carrier systems. *PLoS. One* **2017,** *22*, 12(8), e0183487.
10. Afloarea, O.T.; Cheaburu Yilmaz, C.N.; Verestiuc, L.; Bibire, N. Development of Vaginal Carriers Based on Chi-tosan-Grafted-PNIPAAm for Progesterone Administration. *Gels* **2022,** *8*, 596.

 doi:10.20944/preprints202409.1365.v

11. Cheaburu-Yilmaz, C. N. On the development of chitosan-graft-poly(N-isopropylacrylamide) by RAFT polymerization tech-nique. *Cellul. Chem. Technol.* **2020**, *54* (1-2),1-10.
12. Cheaburu-Yilmaz, C.N.; Yilmaz, O.; Kose, F.A.; Bibire, N. Chitosan-Graft-Poly(N-Isopropylacrylamide)/PVA cryogels as carriers for mucosal delivery of voriconazole. *Polymers* **2019,** *11* (9),1432.
13. Rençber, S.; Cheaburu-Yilmaz, C. N.; Köse, F.A.; Karavana, S.Y.; Yilmaz, O. Preparation and characterization of alginate and chitosan IPC Based Gel Formulation for Mucosal Application. *Cellul. Chem. Technol.* **2019**, *53* (7-8), 655-665.
14. Cheaburu-Yilmaz, C. N.; Lupuşoru, C.E.; Vasile, C. New Alginate/PNIPAAm Matrices for Drug Delivery. *Polymers* **2019,** *11* (2), 366.
15. Mohite, P.; Shah, S.R.; Singh, S.; Rajput, T.; Munde, S.; Ade, N.; Prajapati, B.G.; Paliwal, H.; Mori, D.D.; Dudhrejiy, A.V. Chitosan and chito-oligosaccharide: a versatile biopolymer with endless grafting possibilities for multifarious applications. *Front. Bioeng. Biotechno.l* **2023**, *19*, 1190879.
16. Ward, M.A.; Georgiou, T.K. Thermoresponsive polymers for biomedical applications. *Polymers* **2011**, *3*, 1215-1242.
17. Ansari, M.J.; Rajendran, R.R.; Mohanto, S.; Agarwal, U.; Panda, K.; Dhotre, K.; Manne, R.; Deepak, A.; Zafar, A.; Yasir, M.; Pramanik, S. Poly(N-isopropylacrylamide)-based hydrogels for biomedical applications: A Review of the State-of-the-Art. *Gels* **2022**, *20*, 454.
18. Alvi, M.; Yaqoob, A.; Rehman, K.; Shoaib S.M.; Akash M.S.H. PLGA-based nanoparticles for the treatment of cancer: current strategies and perspectives. *A.A.P.S. Open.* **2022**, *8*, 12.
19. Ritger, P.L.; Peppas, N.A. A simple equation for description of solute release. II Fickian and anomalous release from swellable devices. *J. Control. Release.* **1987**, *5*, 37-42.
20. Panainte, A.D.; Popa, G.; Pamfil, D.; Butnaru, E.; Vasile, C.; Tartau-Mititelu, L.; Gafitanu, C. In vitro characterization of polyvinyl alcohol/chitosan hydrogels as modified release systems for bisoprolol. *Farmacia* **2018**, *66* (1), 44-48.
21. Orsu, P.; Haider, H.Y.; Koyyada, A. Bioengineering for curcumin loaded carboxymethyl guar gum/reduced graphene oxide nanocomposites for chronic wound healing applications. *Int. J. Pharm.* **2021**, *5* (606), 120928.
22. Liang, C.C.; Park, A.Y.; Guan, J.L. In vitro scratch assay: a convenient and inexpensive method for analysis of cell migration in vitro. *Nat. Protoc.* **2007**, *2* (2), 329-33.
23. Henwood, S.Q.; Liebenberg, W.; Tiedt, L.R.; Lötter, A.P.; de Villiers M.M. Characterization of the solubility and dissolution properties of several new rifampicin polymorphs, solvates, and hydrates. *Drug. Dev. Ind. Pharm.* **2001**, 27(10), 1017-1030.
24. Liu, H.; He, Z.Z.; Yu, L.; Ma J.; Jin X.P. Improved solubility and stability of rifampicin as an inclusion complex of acyclic cucurbit[n]uril. *J. Incl. Phenom. Macrocycl. Chem.* **2021**, *101*, 111-120.
25. Rao M.K.; Rao, K.S.V.; Sudhakar, P.; Chowdoji Rao, K.; Subha, M.C.S. Synthesis and Characterization of biodegradable Poly (Vinyl caprolactam) grafted on to sodium alginate and its microgels for controlled release studies of an anticancer drug. *J. App. Pharm. Sci.* **2013**, *3* (06): 061-069.
26. Snejdrova, E.; Loskot, J.; Martiska, J.; Soukup, T.; Prokes, L.; Frolov, V.; Kucera, T. Rifampicin-loaded PLGA nanoparticles for local treatment of musculoskeletal infections: Formulation and characterization. *Int J Drug Deliv Technol* **2022**, 73, 103435.
27. Rai, P.Y.; Sansare, V.A.; Warrier, D.U.; Shinde, U.A. Formulation, characterization and evaluation of inhalable effervescent dry powder of Rifampicin nanoparticles. *Indian J. Tuberc.* **2023**, *70* (1), 49-58.
28. Parmar, R.; Misra, R.; Mohanty, S. In vitro controlled release of Rifampicin through liquid-crystalline folate nanoparticles. *Colloids Surf. B Biointerfaces* **2015**, *1* (129), 198-205.
29. Henwood, S.Q.; de Villiers, M.M.; Liebenberg, W.; Lötter, A.P. Solubility and dissolution properties of generic rifampicin raw materials. *Drug. Dev. Ind. Pharm.* **2000**, *26* (4), 403-408.
30. Khadka, P.; Hill, P.C.; Zhang, B.; Katare, R.; Dummer, J.; Das, S.C. A study on polymorphic forms of rifampicin for inhaled high dose delivery in tuberculosis treatment. *Int. J. Pharm.* **2020**, *25* (587), 119602.
31. Hiremath, S.P.; Saha, R.N. Design and study of rifampicin oral controlled release formulations. *Drug. Deliv.* **2004**, *11* (5), 311-317.
32. Saravanan, P.; Dusthackeer, V.N.A.; Rajmani, R.S.; Mahizhaveni, B.; Nirmal, C.R.; Rajadas, S.E.; Bhardwaj, N.; Ponnuraja, C.; Bhaskar, A.; Hemanthkumar, A.K.; Ramachandran, G.; Tripathy, S.P. Discovery of a highly potent novel rifampicin analog by preparing a hybrid of the precursors of the antibiotic drugs rifampicin and clofazimine. *Sci. Rep.* **2021**, *13*;11(1), 1029.
33. Warheit, D.B.; Oberdörster, G.; Kane, A.B.; Brown, S.C.; Klaper, R.D.; Hurt, R.H. Nanoparticle toxicology. **In** Casarett & Doull's Toxicology: The Basic Science of Poisons, 9th ed.; Klaassen C.D., Ed.; McGraw-Hill Education, 2019, pp. 546-559.
34. Chèvre, N.; Gregorio, V. Mixture effects in ecotoxicology. **In** Encyclopedia of aquatic ecotoxicology; Férard, J.F., Blaise, C, Eds.; Springer, Dordrech, 2013, pp. 671-765.

 doi:10.20944/preprints202409.1365.v

35. Bibire, T.; Dănilă, R.; Yilmaz, C.N.; Verestiuc, L.; Nacu, I.; Ursu, R.G.; Ghiciuc, C.M. In vitro biological evaluation of an alginate-based hydrogel loaded with rifampicin for wound care. Pharmaceuticals **2024**, *17*, 943.
36. Sharma, A.; Puri, V.; Kumar, P.; Singh, I.; Huanbutta, K. Development and evaluation of rifampicin loaded alginate–gelatin biocomposite microfibers. *Polymers* **2021**, *13*, 1514.
37. Papadakis, M. Wound irrigation for preventing surgical site infections. *World J Methodol* **2021**, 20;11(4), 222-227.
38. Gfeller, R.W.; Crowe, D.T. The emergency care of traumatic wounds: current recommendations. *Vet. Clin. North. Am. Small. Anim. Pract.* **1994**, *24* (6), 1249-1274.